Dual RXR motifs regulate nerve growth factor–mediated intracellular retention of the delta opioid receptor

Daniel J. Shiwarski[a,b,†], Stephanie E. Crilly[c,†], Andrew Dates[a], and Manojkumar A. Puthenveedu[a,c,d,*]
[a]Department of Biological Sciences, The Center for the Neural Basis of Cognition, and [b]Department of Biomedical Engineering, Carnegie Mellon University, Pittsburgh, PA 15213; [c]Cellular and Molecular Biology Program, University of Michigan, Ann Arbor, MI 48109; [d]Department of Pharmacology, University of Michigan Medical School, Ann Arbor, MI 48109

ABSTRACT **The delta opioid receptor (DOR), a physiologically relevant prototype for G protein–coupled receptors, is retained in intracellular compartments in neuronal cells. This retention is mediated by a nerve growth factor (NGF)-regulated checkpoint that delays the export of DOR from the *trans*-Golgi network. How DOR is selectively retained in the Golgi, in the midst of dynamic membrane transport and cargo export, is a fundamental unanswered question. Here we address this by investigating sequence elements on DOR that regulate DOR surface delivery, focusing on the C-terminal tail of DOR that is sufficient for NGF-mediated regulation. By systematic mutational analysis, we define conserved dual bi-arginine (RXR) motifs that are required for NGF- and phosphoinositide-regulated DOR export from intracellular compartments in neuroendocrine cells. These motifs were required to bind the coatomer protein I (COPI) complex, a vesicle coat complex that mediates primarily retrograde cargo traffic in the Golgi. Our results suggest that interactions of DOR with COPI, via atypical COPI motifs on the C-terminal tail, retain DOR in the Golgi. These interactions could provide a point of regulation of DOR export and delivery by extracellular signaling pathways.**

Monitoring Editor
Benjamin S. Glick
University of Chicago

Received: May 11, 2018
Revised: Dec 21, 2018
Accepted: Dec 27, 2018

INTRODUCTION

The strength and specificity of signaling via G protein–coupled receptors (GPCRs), which recognize the majority of signals in our bodies, can be regulated directly by changing the number of receptors on cell surfaces. How amino acid sequences and posttranslational modifications on the cytoplasmic regions of GPCRs, as well as extracellular signaling pathways, modulate endocytic removal and reinsertion of surface receptors has been heavily studied (Marchese *et al.*, 2008; Puthenveedu *et al.*, 2010; Magalhaes *et al.*, 2012; Pavlos and Friedman, 2017; Eichel and von Zastrow, 2018).

Regulation of biosynthetic transport of GPCRs is less well explored than endocytic trafficking. The classical view has been that GPCR transport to the cell surface is constitutive and relatively unregulated, with folding and exit from the endoplasmic reticulum (ER) being the limiting steps. Consistent with this view, pharmacological chaperones that enhance folding can increase surface levels of GPCRs (Petäjä-Repo *et al.*, 2002a; Leskelä *et al.*, 2007). Some GPCRs contain diacidic motifs (DXE), dihydrophobic phenylalanine motifs (FF), and di-leucine-containing motifs (LL) that are required for ER exit and might interact with the coatomer protein II (COPII) coat (Duvernay *et al.*, 2004, 2009; Dong *et al.*, 2007; Zhang *et al.*, 2011). Recent data suggest that there are additional requirements for GPCR transport to the cell surface after ER exit. Two sequence motifs—a polybasic motif and a multi-arginine-containing motif—on adrenergic receptors interact with GGA proteins and mediate receptor export from the Golgi, and such sequences might also influence ER exit or ER retrieval (Zhang *et al.*, 2016;

This article was published online ahead of print in MBoC in Press (http://www.molbiolcell.org/cgi/doi/10.1091/mbc.E18-05-0292) on January 2, 2019.

†These authors contributed equally to this work.

*Address correspondence to: Manojkumar A. Puthenveedu (puthenve@umich.edu).

Abbreviations used: COPI, coatomer protein I; COPII, coatomer protein II; DOR, delta opioid receptor; ER, endoplasmic reticulum; GPCR, G protein–coupled receptor; GST, glutathione *S*-transferase; HEK293, embryonic kidney 293 cells; LY, LY294002; NT, no treatment; PC12, pheochromocytoma-12 cells; PI3K, phosphoinositide-3 kinase; PI4P, phosphatidylinositol 4-phosphate; PI(3,4)P2, phosphatidylinositol 3,4-bisphosphate; PKA, protein kinase A; PTEN, phosphatase and tensin homologue; Wort, Wortmannin.

Schutze *et al.*, 1994; Michelsen *et al.*, 2005; Gilbert *et al.*, 2014). Similarly, a lysine-based motif on the delta opioid receptor (DOR) can interact with the coatomer protein I (COPI) coat and cause retention in HEK293 cells (St-Louis *et al.*, 2017). The presence of these sequence elements suggests that GPCR export is an active process. Whether these sequence elements are simply requirements for constitutive trafficking, or can be regulated by extracellular signals, is an important unanswered question.

DOR is a physiologically relevant prototype to address this question (Petaja-Repo *et al.*, 2000; Shiwarski *et al.*, 2017a,b). In neuronal cells, DOR is predominantly localized in intracellular compartments due to a neuron-specific checkpoint that limits export of the receptor from the Golgi apparatus (Kim and von Zastrow, 2003; Shiwarski *et al.*, 2017a,b). In neuroendocrine PC12 cells, this export checkpoint can be triggered acutely by treatment with nerve growth factor (NGF; Kim and von Zastrow, 2003; Shiwarski *et al.*, 2017a). NGF modulates enzymes regulating 3′ phosphoinositide on the *trans*-Golgi network to engage this checkpoint (Shiwarski *et al.*, 2017b). Regulated delivery of DOR from this intracellular compartment to the cell surface can increase surface DOR signaling and antinociception without increasing adverse effects, indicating that regulated retention and delivery are physiologically important (Shiwarski *et al.*, 2017a). Because the last 27 amino acids in the C-terminal tail of DOR were sufficient for NGF-mediated regulation of DOR surface transport (Kim and von Zastrow, 2003; Shiwarski *et al.*, 2017a,b), we hypothesized that NGF regulates the interactions of the C-terminal tail of DOR to regulate Golgi export of DOR.

Here we analyze the sequence elements on the cytoplasmic tail of DOR that were required for NGF-regulated surface transport of DOR, using a strategy of systematic mutagenesis. We identify redundant atypical arginine-based motifs on the C-terminal tail of DOR, corresponding to atypical COPI binding motifs, as required for NGF- or PI3K-regulated intracellular retention of DOR. Such "bibasic" motifs provide a potential way to coordinate COPI-mediated retention of GPCRs in response to specific extracellular signaling pathways, allowing regulated release and surface delivery on demand.

RESULTS

The C-terminal tail of DOR is required for receptor delivery to the cell surface

We started by investigating whether the last 27 amino acids in the C-terminal tail of DOR were required for NGF-mediated regulation of DOR surface transport. We first attempted to delete the entire C-terminal 27 amino acids of DOR, but this resulted in poor surface expression, consistent with the C-terminal tail being required for proper folding and ER export. Therefore, we generated four smaller deletions (Δ345–352, Δ353–359, Δ360–366, Δ367 TGA) of a FLAG-tagged version of the mouse DOR (Figure 1A and Supplemental Figure S1A). PC12 cells were transfected with wild type or an individual deletion mutant and imaged via fixed-cell confocal fluorescence microscopy to determine DOR localization under normal growth conditions and following 1 h of NGF treatment. Wild-type DOR was localized to the surface at baseline and was retained in a Golgi-localized pool following NGF treatment (Figure 1A). The deletion mutants Δ345–352, Δ353–359, Δ360–366, and Δ367 TGA were also surface-localized at baseline and showed noticeable Golgi localization following NGF treatment (Figure 1A). The total levels of DOR were comparable across all conditions, and we and others have established that this Golgi localization is due to a block in export of DOR from the *trans*-Golgi network mediated by the C-terminal tail (Kim and von Zastrow, 2003; Shiwarski *et al.*, 2017a,b).

To quantitate the differences in DOR export between the various deletion mutants, we used a method that we had validated previously to calculate the percentage of total DOR that was retained in the Golgi (Shiwarski *et al.*, 2017a,b). Briefly, we used TGN-38 staining to create a mask defining the Golgi area (*trans*-Golgi network) in the cell. We applied this mask to the receptor channel to quantify receptor signal in the Golgi. This Golgi receptor signal was then expressed as a fraction of total receptor signal in the cell. In addition to this single-cell measure to quantify retention, we also determined the percentage of cells that showed Golgi-localized DOR under each condition at a population level. The data were normalized to the wild-type receptor in the absence of NGF.

In the absence of NGF, all deletion mutants of DOR were localized to the surface, similarly to wild-type DOR. In the presence of NGF, the percentage of total receptor retained in the Golgi increased significantly for all DOR constructs, indicating that none of these regions was fully required for NGF-mediated DOR retention. NGF-induced Golgi localization of DOR was reduced for the Δ345–352 and Δ353–359 receptors compared with wild-type DOR. Similarly, when the percentage of cells with Golgi-localized DOR following NGF was quantitated, fewer cells showed retention of Δ345–352 and Δ353–359 receptors than with wild-type DOR (Figure 1C). These data show that the last 27 amino acids of DOR are required for proper trafficking of the receptor to the cell surface and that the region between amino acids 345 and 359 might play a role in the NGF-induced Golgi localization of DOR. Together with previous data indicating that the C-terminal 27 amino acids are sufficient for NGF-regulated transport of DOR (Kim and von Zastrow, 2003; Shiwarski *et al.*, 2017b), these data implicate the C-terminal tail as being required and sufficient for regulating DOR export

Deletions Δ345–352 and Δ353–359 partially reduce Golgi retention following PI3K inhibition

To ensure that the C-terminal tail was required for the physiologically relevant phosphoinositide-regulated Golgi checkpoint that regulated the surface delivery of DOR in neurons (Shiwarski *et al.*, 2017a,b), we tested whether the Δ345–352 and Δ353–359 deletion mutants reduced Golgi retention of DOR following PI3K inhibition. PC12 cells expressing FLAG-tagged DOR wild type, Δ345–352, and Δ353–359 were treated with the PI3K inhibitor Wortmannin (Wort; 10 μM) or LY294002 (LY; 10 μM) for 1 h and imaged with immunofluorescence to determine DOR localization. As expected, a significant fraction of total wild-type DOR (WT) was localized to the Golgi following PI3K inhibition (Figure 2B). In contrast, less of the Δ345–352 and Δ353–359 DOR was localized to the Golgi following PI3K inhibition (Figure 2B). We evaluated this difference quantitatively by measuring the fraction of DOR that overlapped with the *trans*-Golgi marker TGN-38, as in Figure 1B. Both the Δ345–352 and Δ353–359 deletion mutants demonstrated a small, but statistically significant, reduction in the percentage of DOR localized to the Golgi after treatment with Wortmannin. LY294002 caused a similar reduction, but this was not statistically significant (Figure 2C). Similarly, the Δ345–352 and Δ353–359 deletions resulted in lower percentages of cells with Golgi-localized DOR after PI3K inhibition (Figure 2D). These data suggest that the two regions played partial roles in NGF-induced and PI3K inhibition–induced retention of DOR, raising the possibility that there could be redundant sequences in the C-terminal tail.

Classical diarginine-containing motifs within the cytoplasmic domains are not primary requirements for DOR retention

Because Δ345–352 and Δ353–359 reduced, but did not completely prevent, the NGF and PI3K inhibition–induced Golgi retention of

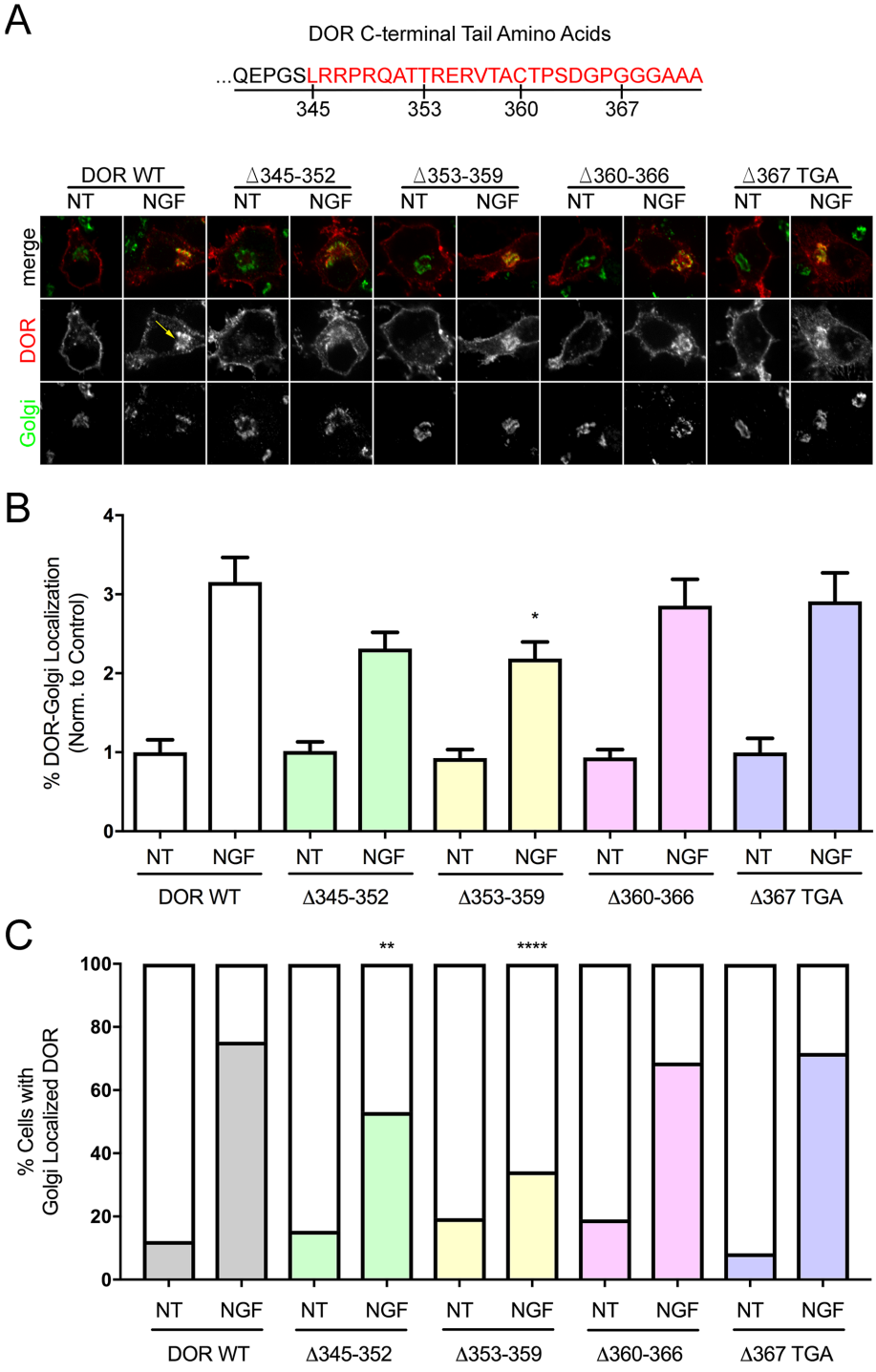

FIGURE 1: The C-terminal tail of DOR regulates delivery of the receptor to the cell surface. (A) The last 27 amino acids of the DOR C-terminal tail were subdivided into four deletion mutants. In a Flag-tagged DOR construct, deletion mutants were made to determine the region within the DOR C-terminal tail required for the NGF-induced Golgi retention of DOR (Δ345–352, Δ353–359, Δ360–366, and Δ367 TGA). In PC12 cells expressing the wild-type Flag-tagged DOR (DOR WT), immunofluorescence images reveal that DOR is highly expressed on the cell surface under control no-treatment (NT) conditions. DOR accumulates in a region that colocalizes with the *trans*-Golgi network marker TGN-38 (yellow arrow) following 1 h of nerve growth factor treatment (NGF, 100 ng/ml). Sectional deletions of the regions comprising the 27 amino acids of the C-terminal DOR tail sequence all demonstrate baseline surface localization under control NT conditions, and accumulation of DOR within the Golgi region following NGF treatment. (B) Quantitative analysis of the immunofluorescence images showed an increase in the percentage of DOR fluorescence localized to the Golgi region following NGF treatment for cells expressing DOR WT. Of the individual DOR tail-deletion mutants, the Δ345–352 and the Δ353–359 both displayed a small reduction in the percentage of DOR fluorescence localized to the Golgi following NGF treatment, with only Δ353–359 showing a significant reduction compared with DOR WT NGF. The remaining deletion mutants were similar to DOR WT under both NT and NGF treatment conditions (DOR WT NT, $n = 82$ cells; DOR WT NGF, $n = 77$ cells; Δ345–352 NT, $n = 97$ cells; Δ345–352 NGF, $n = 98$ cells; Δ353–359 NT, $n = 77$ cells; Δ353–359 NGF, $n = 105$ cells; Δ360–366 NT, $n = 84$ cells; Δ360–366 NGF, $n = 80$ cells; Δ367 TGA NT, $n = 34$ cells; Δ367 TGA NGF, $n = 39$ cells; mean ± SEM; $*p < 0.05$, by one-way ANOVA with Dunnett's multiple comparisons test vs. DOR WT NGF). (C). Additional quantification of the percentage of cells that appeared to have Golgi-localized DOR demonstrated a pattern similar to the fluorescence quantification. The Δ345–352 and the Δ353–359 DOR tail deletions displayed a small, but significant reduction in the percentage of cells with Golgi-localized DOR following NGF treatment compared with DOR WT NGF (DOR WT NT, $n = 82$ cells; DOR WT NGF, $n = 77$ cells; Δ345–352 NT, $n = 97$ cells; Δ345–352 NGF, $n = 98$ cells; Δ353–359 NT, $n = 77$ cells; Δ353–359 NGF, $n = 105$ cells; Δ360–366 NT, $n = 84$ cells; Δ360–366 NGF, $n = 80$ cells; Δ367 TGA NT, $n = 34$ cells; Δ367 TGA NGF, $n = 39$ cells; mean ± SEM; $**p < 0.01$, $****p < 0.0001$; by a two-tailed chi-squared test vs. DOR WT NGF).

DOR, we next attempted to identify sequence elements that were required for DOR retention. We examined potential additional trafficking motifs within DOR. Sequence analysis revealed a diarginine motif in the C-terminal tail (SLRRPR) of DOR (Figure 3A). Because diarginine sequences can facilitate ER retention and COPI retrieval from post-ER compartments and the Golgi (Schutze *et al.*, 1994; Roth *et al.*, 2009), we tested whether such sequences were required for DOR retention. Because a related diarginine sequence (RSLRR) was present in the third intracellular loop of DOR, we mutated all amino acids within each motif to alanine (SLRRPR to AAAAAA and RSLRR to AAAAA).

PC12 cells expressing either a wild-type Flag-tagged DOR or one of the alanine-mutated motif receptors (SLRRPRΔAla, RSLRRΔAla) were treated with NGF or the PI3K inhibitor LY294002 for 1 h as above. Example images from fixed-cell confocal immunofluorescence microscopy showed that all wild-type and mutated receptors demonstrated primarily surface localization under normal baseline no-treatment conditions. NGF and LY294002 treatment increased Golgi localization of DOR compared with

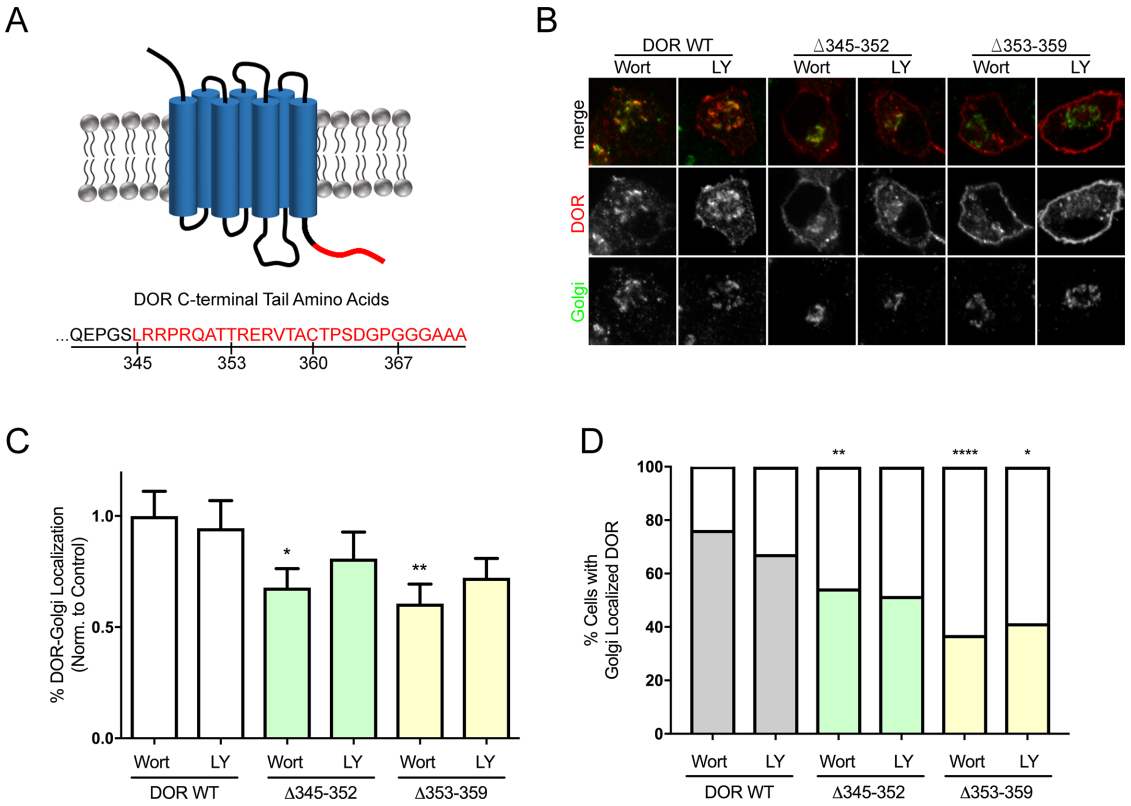

FIGURE 2: The DOR C-terminal tail deletions Δ345–352 and Δ353–359 exhibit a reduction in Golgi retention following PI3K inhibition. (A) Schematic of the delta-opioid receptor topology with the last 27 amino acids of the C-terminal tail identified (red). The amino acid sequence of the C-terminal tail is depicted at the bottom. (B) Immunofluorescence images of the PC12 cells expressing DOR WT, Δ345–352, and Δ353–359 after 1 h of treatment with the PI3K inhibitor Wortmannin (Wort; 10 μM) or LY294002 (LY; 10 μM). The Δ345–352 and Δ353–359 deletion mutants both displayed less DOR fluorescence localized to the Golgi than DOR WT. (C) Quantification of the percentage of DOR fluorescence localized to the Golgi was normalized to DOR WT with Wortmannin to compare the deletion mutants with the full-length DOR. For both the Δ345–352 and Δ353–359 deletions after treatment with Wortmannin, a small, but statistically significant reduction in the percentage of DOR localized to the Golgi was observed (DOR WT Wort, $n = 76$ cells; DOR WT LY, $n = 55$ cells; Δ345–352 Wort, $n = 79$ cells; Δ345–352 LY, $n = 62$ cells; Δ353–359 Wort, $n = 73$ cells; Δ353–59 LY, $n = 50$ cells; mean ± SEM; $^*p < 0.05$, $^{**}p < 0.01$, by one-way ANOVA with Dunnett's multiple comparisons test vs. DOR WT, Wort or LY). (D) Similarly, the Δ345–352 and Δ353–359 deletions resulted in a lower percentage of cells with Golgi-localized DOR after treatment with Wortmannin. Following treatment with LY294002, only the Δ353–359 was significantly reduced compared with the DOR WT (DOR WT Wort, $n = 76$ cells; DOR WT LY, $n = 55$ cells; Δ345–352 Wort, $n = 79$ cells; Δ345–352 LY, $n = 62$ cells; Δ353–359 Wort, $n = 73$ cells; Δ353–359 LY, $n = 50$ cells; mean ± SEM; $^*p < 0.05$, $^{**}p < 0.01$, $^{****}p < 0.0001$, by two-tailed chi-squared test vs. DOR WT, Wort or LY).

the control no-treatment conditions for all DOR constructs (Figure 3B). When the images were analyzed as above, the SLRRPRΔAla and RSLRRΔAla did not change the fraction of Golgi-localized DOR following NGF. Mutating the SLRRPRΔAla and RSLRRΔAla individually caused a small, but significant, decrease in DOR fluorescence within the Golgi following PI3K inhibition by LY294002 (Figure 3C). Similarly, analysis of the percentage of cells with Golgi-localized DOR showed a nonsignificant decrease for SLRRPRΔAla and RSLRRΔAla alone following NGF treatment. A small but significant decrease was observed between the DOR WT LY294002 and the SLRRPRΔAla and RSLRRΔAla alone (Figure 3D). These data suggest that the diarginine motifs are not the primary determinants for NGF-induced DOR retention.

Atypical COPI-binding RXR motifs within the C-terminal tail of DOR mediate NGF-induced Golgi retention

Amino acid sequences containing arginine (R)–any amino acid (X)–arginine (R), or RXR, motifs can retain ion channels in the endoplasmic reticulum (Zerangue *et al.*, 1999; Ma *et al.*, 2001). Because the C-terminal 27 amino acids of DOR were sufficient for regulated DOR retention and delivery (Kim and von Zastrow, 2003; Shiwarski *et al.*, 2017b), we checked whether this region contained similar sequence motifs. By evaluating the evolutionary conservation of the DOR (oprd1 gene) C-terminal tail across human, mouse, and rat species, we identified two highly conserved RXR motifs, 347–349 (RPR) and 354–356 (RER; Figure 4A). Because the two deletions (Δ345–352 and Δ353–359; Figure 1) and alanine mutants that removed these motifs one at a time showed only partial reduction in retention (SLRRPRΔAla and TTRERΔAla; Figure 3 and Supplemental Figure S1), we mutated all five arginine residues present in these two regions to alanines. When expressed in PC12 cells, under baseline conditions, these mutant receptors (DOR) were localized to the cell surface at levels comparable to wild-type receptors. Example images from fixed-cell confocal immunofluorescence imaging of PC12 cells expressing either wild-type Flag-tagged DOR or RXR mutant DOR (DOR 2AXA) are shown in Figure 4B. Following NGF

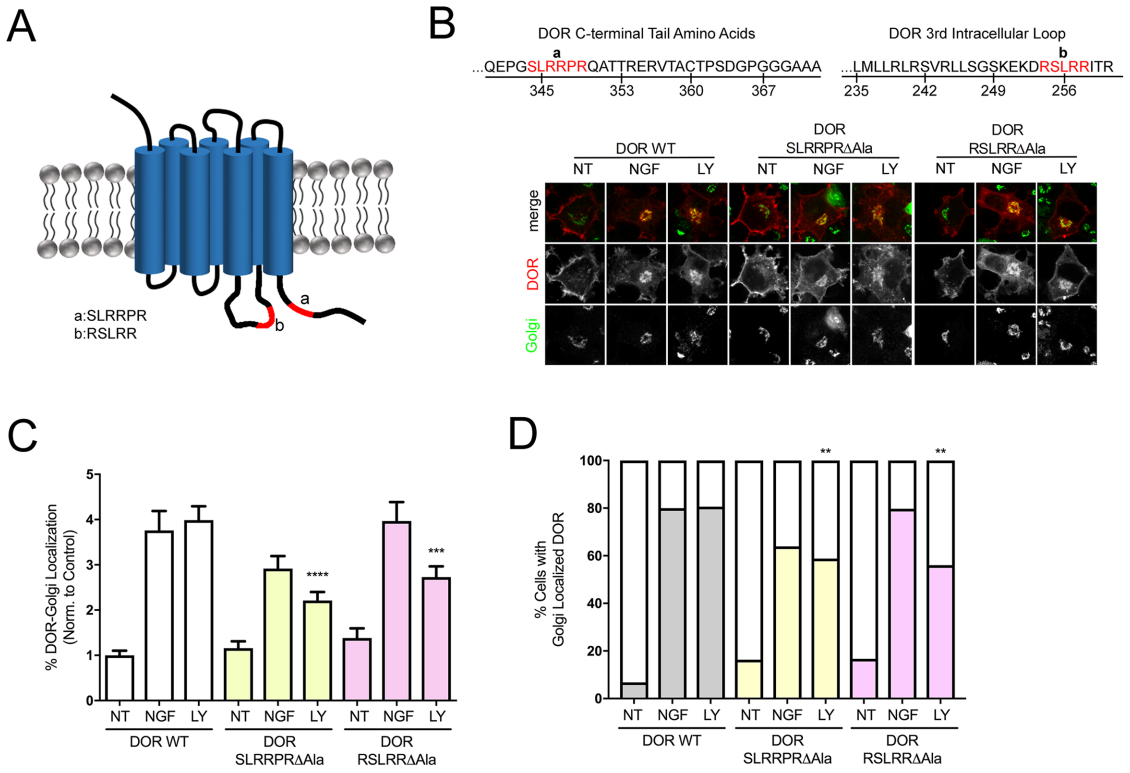

FIGURE 3: Diarginine motifs in the third intracellular loop and C-terminal tail of DOR are not required for NGF-induced DOR retention. (A) Alanine mutant versions of a Flag-tagged DOR were made containing SLRRPR to AAAAAA (a) and RSLRR to AAAAA (b). (B) Immunofluorescence imaging of PC12 cells expressing a wild-type Flag-tagged DOR (DOR WT) or alanine mutated diarginine containing motifs demonstrated primarily surface localization under normal baseline no-treatment conditions (NT). Following NGF treatment for 1 h (NGF; 100 ng/ml) or PI3K inhibition by LY294002 (LY; 10 μM), all DOR constructs exhibited increased Golgi localization. (C) Quantification of the percentage of DOR fluorescence localized to the Golgi was normalized to DOR WT with NT to compare the alanine-mutated diarginine-containing motifs with the full-length DOR. Mutating the SLRRPRΔAla and RSLRRΔAla did not significantly affect the NGF-induced DOR-Golgi localization. Mutating the SLRRPRΔAla and RSLRRΔAla alone resulted in a significant decrease in the DOR fluorescence within the Golgi following PI3K inhibition by LY compared with DOR WT LY (DOR WT NT, $n = 58$ cells; DOR WT NGF, $n = 56$ cells; DOR WT LY, $n = 67$ cells; SLRRPRΔAla NT, $n = 49$ cells; SLRRPRΔAla NGF, $n = 91$ cells; SLRRPRΔAla LY, $n = 85$ cells; RSLRRΔAla NT, $n = 40$ cells; RSLRRΔAla NGF, $n = 52$ cells; RSLRRΔAla LY, $n = 91$ cells; mean ± SEM; ***$p < 0.001$, ****$p < 0.0001$, by one-way ANOVA with Dunnett's multiple comparison test vs. DOR WT, NGF and LY). (D) Analysis of the percentage of cells with Golgi-localized DOR showed a small but significant decrease between the DOR WT LY and the SLRRPRΔAla and RSLRRΔAla alone (DOR WT NT, $n = 58$ cells; DOR WT NGF, $n = 56$ cells; DOR WT LY, $n = 67$ cells; SLRRPRΔAla NT, $n = 49$ cells; SLRRPRΔAla NGF, $n = 91$ cells; SLRRPRΔAla LY, $n = 85$ cells; RSLRRΔAla NT, $n = 40$ cells; RSLRRΔAla NGF, $n = 52$ cells; RSLRRΔAla LY, $n = 91$ cells; mean ± SEM; **$p < 0.01$, by two-tailed chi-squared test vs. DOR WT, NGF and LY).

treatment, or PI3K inhibition by LY294002 for 1 h, the arginine mutant was surface localized, unlike wild-type DOR, which was retained in intracellular compartments as expected (Figure 4B). When quantified, DOR 2AXA showed a significant decrease in the fraction of receptors that overlapped with the Golgi marker TGN-38 (Figure 4C) and the number of cells showing intracellular retention after NGF or LY treatment (Figure 4D). Because deletion and alanine substitution of these regions individually did not fully inhibit retention, it is likely that these two RXR motifs are partially redundant.

RXR motifs in the DOR C-terminal tail are required and sufficient for interaction with COPI

Given that these RXR motifs were required for DOR retention, we next asked whether these residues served as interacting motifs for machinery that could cause cargo to localize to the Golgi by retention or retrieval. Because RXR motifs in ion channels were originally described as binding COPI and retrieving unassembled subunits to the ER (Zerangue *et al.*, 1999; Ma *et al.*, 2001; Yuan *et al.*, 2003), we focused on COPI as a potential interacting factor for the DOR RXR motifs. We addressed whether DOR binds COPI by immunoprecipitating Flag-tagged DOR and DOR 2AXA and immunoblotting for the Beta-COP subunit of coatomer. As shown in Figure 5A, Beta-COP coimmunoprecipitated with wild-type DOR, suggesting that they interact in cells. We observe a significant decrease in Beta-COP coimmunoprecipitation with DOR 2AXA compared with wild-type DOR (Figure 5, A and B). We did not see a complete loss of binding, consistent with a conventional lysine-based motif in an intracellular loop of DOR that was identified as binding COPI (St-Louis *et al.*, 2017), but the reduction in Beta-COP coimmunoprecipitation suggests that the RXR motif contributes to COPI binding.

Therefore, we next used an affinity purification approach to test whether C-terminal RXR motifs were sufficient for interaction with COPI machinery. PC12 cell lysate was incubated with GST fusion proteins consisting of either GST fused to the last 27 amino acids of

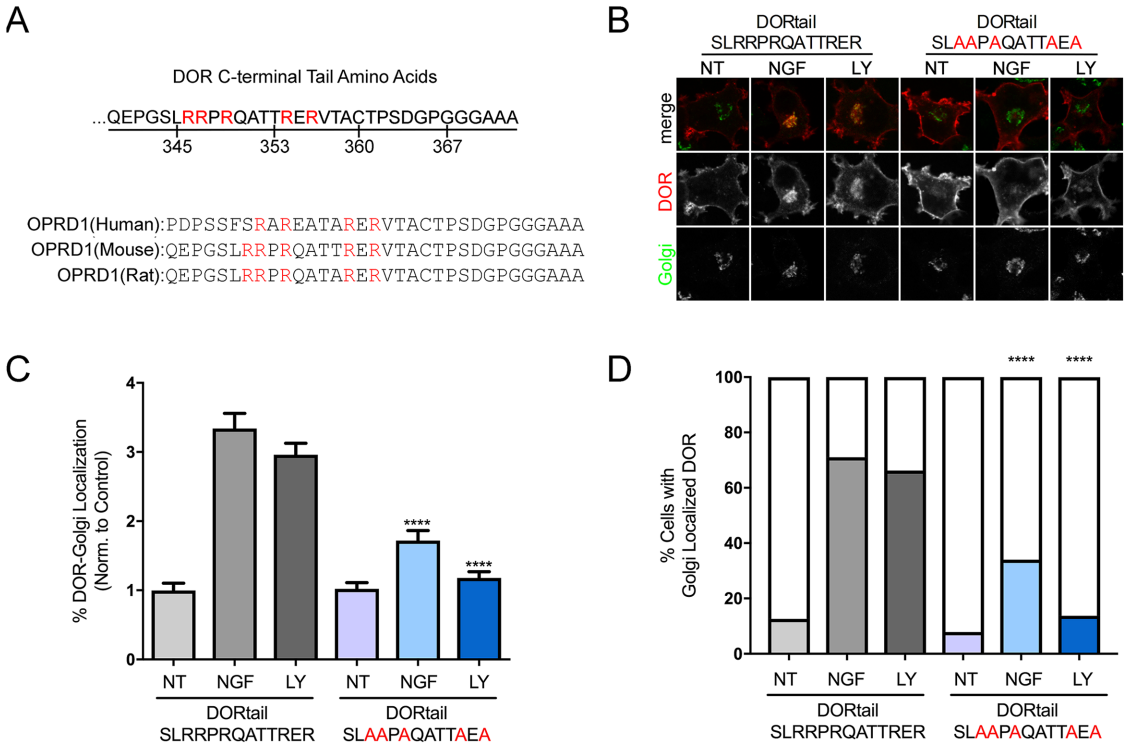

FIGURE 4: Dual RXR motifs within the C-terminal tail of DOR are required for NGF-induced Golgi retention. (A) The C-terminal 27 amino acids of DOR contain two highly conserved RXR retention motifs. Sequence comparison between the human, mouse, and rat DOR (OPRD1) C-terminal tail demonstrates high sequence conservation (arginine highlighted in red). All five of the arginine within the mouse C-terminal tail of DOR were mutated to alanine. (B) Immunofluorescence imaging of PC12 cells expressing a wild-type Flag-tagged DOR (DORtail SLRRPRQATTRER) or alanine-mutated RXR motifs (DORtail SLAAPAQATTAEA) demonstrated primarily surface localization under normal baseline no-treatment conditions (NT). Following NGF treatment for 1 h (NGF; 100 ng/ml), or PI3K inhibition by LY294002 (LY; 10 μM), wild-type DOR exhibited increased Golgi localization; however, the arginine mutant was almost completely surface-localized. (C) Quantification of the percentage of DOR fluorescence localized to the Golgi was normalized to wild-type DOR (DORtail SLRRPRQATTRER) NT to compare the alanine-mutated RXR motifs (DORtail SLAAPAQATTAEA) with the full-length DOR. Mutating the RXR motifs (DORtail SLAAPAQATTAEA) significantly decreased the NGF and LY-induced DOR-Golgi localization (DORtail SLRRPRQATTRER NT, $n = 86$ cells; DORtail SLRRPRQATTRER NGF, $n = 75$ cells; DORtail SLRRPRQATTRER LY, $n = 159$ cells; DORtail SLAAPAQATTAEA NT, $n = 87$ cells; DORtail SLAAPAQATTAEA NGF, $n = 94$ cells; DORtail SLAAPAQATTAEA LY, $n = 123$ cells; mean ± SEM; ****$p < 0.0001$, by two-sided Student's t test vs. DOR WT, NGF and LY). (D) Further analysis of the percentage of cells with Golgi-localized DOR showed a significant decrease between the DOR WT NT and LY and the RXR motifs mutant (DORtail SLAAPAQATTAEA; DORtail SLRRPRQATTRER NT, $n = 86$ cells; DORtail SLRRPRQATTRER NGF, $n = 75$ cells; DORtail SLRRPRQATTRER LY, $n = 159$ cells; DORtail SLAAPAQATTAEA NT, $n = 87$ cells; DORtail SLAAPAQATTAEA NGF, $n = 94$ cells; DORtail SLAAPAQATTAEA LY, $n = 123$ cells; mean ± SEM; ****$p < 0.0001$, by two-tailed chi-squared test vs. DOR WT, NGF and LY).

the DOR C-terminal tail (GST-DOR) or a mutant in which the five arginine residues in the tail were mutated to alanines (GST-2AXA). Beta-COP copurified with the GST-DOR but not with GST-2AXA or GST alone, at 10- and 3.3-μM concentrations, as shown by immunoblotting for Beta-COP (Figure 5C and Supplemental Figure S2). This showed that the DOR C-terminal tail was sufficient to bind COPI and that the RXR motif was needed to bind Beta-COP in this context. Together, our results suggest a model where RXR motifs in the C-terminal tail of DOR, by binding the COPI retrograde trafficking machinery, regulate the export of DOR from the Golgi in response to extracellular signals.

DISCUSSION

Here, we demonstrate that regulated retention and delivery of DOR require two bi-arginine motifs (RXR) within DOR's C-terminal tail. These RXR motifs are required for interactions of DOR with COPI and for NGF- and PI3K-mediated retention of DOR in the Golgi. This suggests a model where signaling-mediated regulation of receptor interactions with COPI controls the export and surface delivery of DOR from the Golgi.

Regulation of surface delivery of receptors from the biosynthetic pathway is a physiologically relevant step for regulating DOR signaling. Unlike many other GPCRs, such as beta-2 adrenergic receptor or the mu opioid receptor, which are recycled after they are internalized (Puthenveedu *et al.*, 2010; Vistein and Puthenveedu, 2013; Bowman and Puthenveedu, 2015; Bowman *et al.*, 2015; Weinberg *et al.*, 2017), a large fraction of activated DOR is sorted to the lysosome and degraded (Whistler *et al.*, 2002; Henry *et al.*, 2011). Therefore, recovery of cellular sensitivity to DOR agonists depends on the delivery of newly synthesized receptors from the biosynthetic pathway. Consistent with this, membrane-permeable opioid ligands acting as pharmacological chaperones increase the rate of DOR folding and exit from ER in cultured fibroblasts, suggesting that ER exit is the rate-limiting step for surface delivery of DOR in these cells

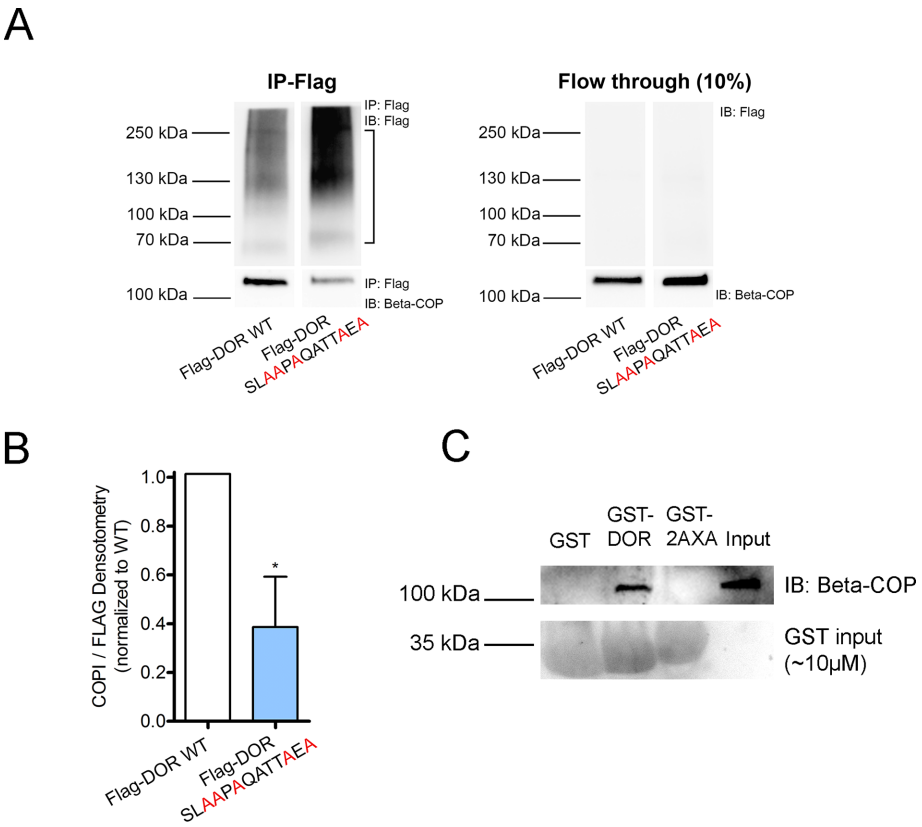

FIGURE 5: DOR C-terminal RXR motifs are required and sufficient for interaction with Beta-COP. (A) PC12 cells expressing Flag-DOR WT or Flag-DOR SLAAPAQATTAEA were cross-linked with 0.5 mM DSP, which was followed by immunoprecipitation (IP) with an anti-Flag antibody and immunoblotting (IB) for Beta-COP or Flag. Immunoblotting for Beta-COP shows more Beta-COP interacting with Flag-DOR WT. Immunoblotting for Flag indicates expression of the tagged receptor and efficient depletion of the tagged receptor from the supernatant after immunoprecipitation. (B) The difference in Beta-COP associated with the WT and mutant receptor quantitate by densitometry. Beta-COP in the IP was normalized to Flag-receptor. The region used for quantitation is noted by square brackets. There was a statistically significant decrease in the amount of Beta-COP that immunoprecipitated with Flag-DOR SLAAPAQATTAEA compared with Flag-DOR WT ($n = 3$, mean ± SEM; $*p < 0.05$ by Student's t test). (C) PC12 cell lysate was incubated with 150 μg (~10 μM) GST fusion proteins bound to glutathione agarose beads, followed by immunoblotting (IB) for Beta-COP. The 110-kDa band corresponding to Beta-COP coprecipitates with the wild-type DOR tail (GST-DOR), but not with GST or the tail lacking RXR motifs (GST-2AXA). Beta-COP is also present in 10 μg whole-cell lysate (Input). A Ponceau-S staining for the respective GST proteins is shown at the bottom. There was no Beta-COP signal above background for GST and GST-2AXA in three separate experiments. A representative image is shown.

(Petaja-Repo *et al.*, 2000, 2002b; Leskelä *et al.*, 2007). In neuronal cells, however, DOR is localized in intracellular compartments after export from the ER, although the amount of DOR retained and the identity of these compartments vary between cell types and experimental approaches (Roth *et al.*, 1981; Cahill *et al.*, 2001; Wang and Pickel, 2001; Bao *et al.*, 2003; Kim and von Zastrow, 2003; Patwardhan *et al.*, 2005; Mittal *et al.*, 2013; Shiwarski *et al.*, 2017a,b). In peripheral neurons, DOR is retained in a post-ER compartment that roughly overlaps with the Golgi apparatus, and this retention is regulated by a signaling pathway involving PI3K and PTEN—enzymes that regulate the conversion of PI4P to PI(3,4)P_2 (Shiwarski *et al.*, 2017a,b). Engineered relocation of DOR from these intracellular compartments increases the amount of functional DOR on the neuronal surface and significantly increases the potency of SNC80 in a mouse model for chronic pain (Shiwarski *et al.*, 2017a). These data suggest that in neurons, the rate-limiting step for surface delivery of DOR is the export from these intracellular storage compartments, and that retention and release of DOR from these compartments have physiological consequences. Our results indicate that retention of DOR in these compartments is mediated by interactions of the DOR with COPI. This provides a potential control point for physiologically relevant regulation of DOR surface delivery.

Our identification of RXR motifs that mediate Golgi retention of DOR suggests that these "atypical" arginine-based motifs can play roles in diverse trafficking steps of multiple cargo. RXR motifs were first shown to mediate retrieval and retention of the ATP-sensitive potassium channel α (Kir6.1/2) and β (SUR1) subunits in the endoplasmic reticulum (ER; Zerangue *et al.*, 1999; Ma *et al.*, 2001). Complete assembly of subunits masks the RXR sequence and allows channel export from the ER. Amino acids between and flanking the arginine residues influenced the magnitude of retention and the compartment within which the channel was retained (Zerangue *et al.*, 2001; Michelsen *et al.*, 2005). RXR motifs also play roles in export of other proteins, such as the vasopressin V2 receptor, the GABA receptor, and the NMDA receptor from the ER depending on protein folding state, dimerization, or phosphorylation (Margeta-Mitrovic *et al.*, 2000; Scott *et al.*, 2001; Hermosilla *et al.*, 2004). Unlike these proteins, however, DOR is properly folded and readily exits the ER irrespective of the RXR motif (Figure 1A). The primary role of RXR motifs in DOR might be in signal-regulated retention in the late Golgi, from which regulated delivery to the surface can cause physiological changes in DOR signaling and antinociception (Shiwarski *et al.*, 2017a,b).

Active retention of cargo in the late Golgi or the *trans*-Golgi network presents an interesting challenge for cargo, considering the prevalent model that each compartment in the Golgi apparatus matures, and cargo transits and exits the Golgi as a "default" mechanism. Our results suggest that DOR is retained by a similar mechanism by which Golgi resident enzymes are retained in the Golgi—by constant COPI-mediated retrieval to earlier compartments. Consistent with this, the RXR motif on COPI was needed to bind COPI. RXR motifs on ion channel subunits and GPCRs have been reported to bind components of the COPI machinery and are sufficient to cause retention of proteins along the secretory pathway in the ER and Golgi (Zerangue *et al.*, 1999, 2001; Yuan *et al.*, 2003; Brock *et al.*, 2005; Michelsen *et al.*, 2005). RXR-mediated interaction of other GPCRs, such as GABAB1 and PAR4, with COPI components via these motifs localize these proteins to the ER (Hermosilla *et al.*, 2004; Brock *et al.*, 2005; Cunningham *et al.*, 2012). For DOR, the COPI interactions could be a mechanism to constantly retrieve receptors from the *trans*-Golgi network to earlier Golgi compartments, allowing retention in the Golgi. Recently,

in HEK293 cells, DOR was shown to interact constitutively with COPI using a traditional dilysine sequence in the intracellular loop that retained DOR in the Golgi (St-Louis *et al.*, 2017). In our experiments, the majority of DOR was delivered to the cell surface under basal conditions. Although it is possible that some amount of DOR was retained in the Golgi at baseline, this retention was significantly increased by NGF treatment or PI3K inhibition (Shiwarski *et al.*, 2017a,b). Further, this retention was abolished in receptors lacking the RXR motifs. It is interesting to note that Wortmannin and LY differed in the extent of effects, although the trends were consistent. This difference is likely due to the diversity in specificity, efficacy, bioavailability, and mechanism of inhibition of these inhibitors on different PI3K isoforms (Powis *et al.*, 1994; Domin *et al.*, 1997; Brown *et al.*, 1999; Knight, 2011). We have previously shown that DOR retention is mediated by Class II alpha PI3K (PI3K C2A) and not the canonical class I PI3K (Shiwarski *et al.*, 2017b), and that higher doses of Wortmannin and LY are needed to cause DOR retention because they are much less effective at inhibiting PI3K C2A than the class I PI3Ks (IC_{50} of 420 nM vs 5 nM for Wortmannin, and 19 µM vs. 0.8 µM for LY; Domin *et al.*, 1997; Brown *et al.*, 1999). Irrespective of these differences in specificity and effectiveness, our results indicate that the interaction of the RXR motif with COPI that we identify here is regulated by extracellular signaling pathways that use PI3K. Such signaling-mediated regulation of COPI interaction could provide a method for cells to fine tune the delivery of DOR to the cell surface in neuronal cells.

How could signals regulate the interactions of the RXR motif with COPI? One possibility is that a regulated interaction of DOR with another as yet unidentified protein could mask the COPI interaction. RXR motifs can be masked by binding of proteins such as 14-3-3 or PDZ-interacting proteins in the vicinity of the RXR C-terminal motifs (Yuan *et al.*, 2003; Michelsen *et al.*, 2005). DOR does not contain a PDZ ligand, but a complement of proteins that interact with its C-terminal tail have been identified (Georgoussi *et al.*, 2012). This could include canonical interacting proteins such as β-arrestins or G proteins (Georgoussi *et al.*, 2012). While there is little direct evidence that these proteins associate with DOR in a regulated manner on the Golgi, this provides an exciting possibility of coupling local signaling to release. Another possibility is that the RXR motif could be masked by dynamic oligomerization of DOR. Dimerization can control ER export and surface trafficking of some GPCRs (Margeta-Mitrovic *et al.*, 2000; Salahpour *et al.*, 2004; Décaillot *et al.*, 2008; Cunningham *et al.*, 2012). For DOR, while it can form homodimers and heterodimers with other GPCRs, and while the C-terminal tail might play a role in this, most of this has been shown at the cell surface (Cvejic and Devi, 1997; Jordan and Devi, 1999; McVey *et al.*, 2001; Law *et al.*, 2005; Gendron *et al.*, 2016). It is also possible that posttranslational modification of the DOR tail could modulate interaction with a masking protein or with COPI. Constitutive palmitoylation of the DOR tail has been implicated in DOR surface expression, whereas reversible palmitoylation and phosphorylation of the tail have been studied at the level of surface receptor activation and internalization (Petäjä-Repo *et al.*, 2006; Gendron *et al.*, 2016). Regulation of COPI interactions by signaling pathways has been reported for the Kir6.2 channel. PKA activation via adrenergic receptors dynamically modulates RXR interaction with COPI and surface expression of the SUR1/Kir6.2 channel (Arakel *et al.*, 2014). Together with our results, this raises the possibility that signaling-mediated regulation of COPI interactions could be a general method for controlling surface delivery of many different proteins.

Regulated Golgi retention and trafficking provide a potential mechanism for cells to fine tune signaling at multiple levels. For "single-use" receptors such as DOR, which are mostly degraded after internalization, a pool of newly synthesized ready-to-use receptors allows rapid "just-in-time" delivery of defined amounts of receptors to the cell surface on demand, by masking the RXR motif. There is also increasing evidence that GPCRs can signal from intracellular compartments such as endosomes and the Golgi, with different consequences than for signaling from the plasma membrane (Irannejad *et al.*, 2013, 2017; Bowman *et al.*, 2016; Stoeber *et al.*, 2018). While it is not yet clear whether DOR generates a physiologically relevant signal from the Golgi, it is possible that regulated interactions of the RXR motif with COPI could modify spatially restricted signaling. While there are several exciting possibilities for the role of the intracellular pool of DOR, it is clear that regulated retention and release play a physiological role in vivo in controlling opioid physiology (Bao *et al.*, 2003; Cahill *et al.*, 2003; Kim and von Zastrow, 2003; Patwardhan *et al.*, 2005; Bie *et al.*, 2010; Mittal *et al.*, 2013; Pettinger *et al.*, 2013; Shiwarski *et al.*, 2017a). Understanding how RXR-motif interactions are regulated could provide strategies for pharmacologically manipulating them and driving functional receptors to the cell surface to modify cellular responses to signals.

MATERIALS AND METHODS

Cell culture and transfection

The cell line used for experimentation was pheochromocytoma-12 (PC12; #CRL-1721) cells grown and cultured in F12K medium (Life Technologies 21127-022) supplemented with 10% horse serum and 5% fetal bovine serum (FBS) at 37°C with 5% CO_2. The medium was changed every 3 d to maintain proper cell health. Tissue culture flasks were coated with collagen IV (Sigma #C5533-5MG) to allow PC12 cells to adhere. Cells were passed at a ratio of 1:4 to ensure sufficient seeding density to facilitate growth. Cells were plated onto collagen IV–coated six-well plates and grown in 10% horse serum and 5% fetal bovine serum F12K media for 24 h before transfection. Cells were transiently transfected using the Lipofectamine 2000 lipofection reagent (Invitrogen 11668-019) with the desired DOR plasmid constructs as previously reported (Shiwarski *et al.*, 2017a,b). DNA and Lipofectamine ratios (7.5 µl of Lipofectamine 2000 and 1.5 µg of the appropriate DOR plasmid DNA) were selected from the manufacturer's recommendations. Cells were left to incubate with the transfection mixture and Opti-MEM for 5 h at 37°C, and the medium was then replaced. Experiments were conducted 48–72 h following transfection.

DNA plasmids and mutagenesis

The wild-type DOR construct consists of an N-terminal signal sequence FLAG-tag in the pcDNA3.1 vector. All point mutants and deletion mutants were constructed using a modified QuickChange PCR protocol and confirmed via DNA sequencing. Primers for the alanine point mutants and deletion mutants were designed using the QuickChange Primer Design Tool from Agilent Technologies. Following the PCR with PfuTurbo high-fidelity polymerase (Agilent Technologies), a *Dpn*I digest was performed for 1 h, followed by bacterial transformation in *Escherichia coli* DH5α (Invitrogen). GST fusion protein plasmids were constructed from GST fused to the last 27 amino acids of DOR in the pGEX-4T1 vector. Alanine mutations were introduced into this construct via a QuickChange PCR protocol and confirmed via DNA sequencing.

Fixed cell immunofluorescence

PC12 cells expressing FLAG-DOR and the FLAG-DOR mutants were plated on coverslips (Corning) coated with poly-D-lysine (Sigma, #P7280) and grown at 37°C for 48 h. Following treatments with

Compound name	Protein target	Concentration	Supplier	Catalogue #
Nerve growth factor	TrkA	100 ng/ml	BD Biosciences	356004
LY294002	PI3K inhibitor	10 μM	Tocris Bioscience	1130
Wortmannin	PI3K inhibitor	10 μM	Enzo Life Sciences	BML-ST415

TABLE 1: Growth factors and inhibitors.

either NGF (100 ng/ml) or PI3K inhibition (LY294002; 10 μM) for 1 h (see Table 1), cells were fixed in 4% paraformaldehyde, pH 7.4. The coverslips were blocked with 1 mM calcium– and 1 mM magnesium–containing phosphate-buffered saline (PBS) with 5% fetal bovine serum, 5% 1 M glycine, and 0.75% Triton X-100. For immunofluorescence imaging, DOR and the *trans*-Golgi network were labeled for 1 h in blocking buffer with anti-FLAG M1 antibody (Sigma-Aldrich #F3040; 1:1000) conjugated with Alexa-647 (Molecular Probes #A20186) and anti–TGN-38 rabbit polyclonal antibody (1:1000; Sigma-Aldrich #T9826), respectively. Alexa-568 goat anti-rabbit secondary (1:1000; Sigma-Aldrich #A11011) antibody in blocking buffer was added for 1 h to label the anti–TGN-38. Cover slips were again washed in calcium–magnesium PBS and mounted on glass slides using Prolong Diamond Reagent (Molecular Probes #P36962). Cells were imaged using an Andor confocal imaging system (XDi spinning disk, Andor) at 60× magnification (Nikon CFI APO TIRF) on a Nikon TE-2000 inverted microscope with a mechanical Piezo XYZ-stage (Nikon), iXon 897 Ultra cameras (Andor), a laser combiner (Andor) containing 405-, 488-, 515-, 568-, and 647-nm excitation capabilities, IQ2 imaging software (Andor), and an isolation table (TMC). The fluorescence ratio was quantified for all cells imaged and averaged to ensure that results were representative of the population.

Image analysis and quantification

All imaging analysis and data were quantified using ImageJ. Custom macros using Golgi staining as a mask were written to allow unbiased measurements for the total DOR fluorescence for each cell and the fluorescence intensity of DOR within the Golgi for fixed and live cell analysis (Shiwarski *et al.*, 2017a). The ratio of DOR fluorescence within the Golgi to total cell fluorescence was used to measure the amount of total DOR in the Golgi under each treatment condition. This ratio was calculated for each cell and then averaged across all cells. Further, the percentage of cells that visually displayed Golgi-localized DOR was manually determined by binary quantification (1 = retention, 0 = no retention). The binary quantification results were averaged to determine the population percentage of cells with Golgi-localized DOR. A more detailed procedure and a quantification example can be found in our previous publication (Shiwarski *et al.*, 2017a).

Immunoprecipitation, immunoblotting, and densitometry

PC12 cells were grown in 10-cm plates and transfected as described above using 5 μg Flag-DOR or Flag-DOR R to A DNA and 37.5 μl Lipofectamine 2000 per plate. Two days after transfection, plates were washed with PBS before being cross-linked with 0.5 mM dithiobis succinimidyl propionate (DSP) for 2 h at 4°C. DSP was then quenched with 20 mM Tris, pH 7.4. Cells were scraped from the plate and incubated in lysis buffer (0.5% Triton X-100, 10 mM HEPES, 150 mM NaCl, 1 mM egtazic acid [EGTA], 0.1 mM MgCl2, pH 7.4, with 1 mM PMSF and Pierce protease inhibitor tab EDTA-free) on ice for 30 min with intermittent vortexing. Lysate was then spun at 13,200 × *g* for 15 min. A Pierce BCA Assay kit was used for protein estimation. ThermoFisher sheep anti-mouse immunoglobulin G dynabeads (30 μl) were prepared for immunoprecipitation by incubating them for 2 h at room temperature with 1 μg Sigma mouse anti-Flag M2 antibody. Prepared beads were rotated with 0.5–1.0 μg/μl PC12 cell lysate, fixed across conditions for each experiment, overnight at 4°C. The next day, beads were washed six times in a solution of 0.1% Triton, 10 mM HEPES, 150 mM NaCl, 1 mM EGTA, 0.1 mM MgCl2, pH 7.4. Elution was carried out in 20 μl lysis buffer with 1 mg/ml Flag peptide for 2 h with gentle agitation at 4°C.

Samples were prepared for SDS–PAGE with reducing sample buffer (RSB) containing fresh 10% beta-mercaptoethanol (BME), and 1 μl 1 M dithiothreitol (DTT) was added to each sample before it was heated at 75°C for 5 min. Proteins were transferred to a nitrocellulose membrane overnight at 4°C. Blots were blocked in 5% milk-TBST solution. Primary antibodies—anti–Beta-COP D10 or Bethyl anti-Flag from Santa Cruz—were used at concentrations of 1:200 and 1:1000, respectively. Secondary goat anti-mouse and anti-rabbit were used at concentrations of 1:1000. Blots were developed with BioRad Clarity Western ECL Substrate and imaged using the BioRad ChemiDoc Touch imager and ThermoScientific iBrightFL1000. Between immunoblotting for Beta-COP and Flag, blots were stripped for 30 min at room temperature and reblocked in 5% milk-TBST for 1 h. ImageLab software (BioRad) was used for densitometry. For Beta-COP, densitometry was performed on the band migrating at 110 kDa. Beta-COP levels were normalized to densitometric measurements of Flag-DOR, which was quantified as the volume between 70 and 250 kDa. Values were plotted using GraphPad Prism 5 software.

GST pull down

GST fusion proteins were bound to glutathione magnetic agarose (Pierce #78601) as recommended by the manufacturer. Beads were washed three times with wash buffer of 1:1 TBS:lysis buffer (10 mM Tris-HCl, 50 mM NaCl, 1 mM EDTA, 10% glycerol, 0.5% Triton X-100, 2 mM DTT, and EDTA-free Pierce protease inhibitor, pH 7.4). GST fusion protein (150 μg) was incubated with beads with rotation for 2 h at 4°C. Beads were washed five times, and then 150 μg PC12 cell lysate prepared using lysis buffer was added and the beads were incubated an additional 2 h at 4°C with rotation. Beads were washed five times with lysis buffer and then resuspended in RSB and heated for 5 min at 95°C to elute proteins. Samples were then analyzed by SDS–PAGE and immunoblotting.

Recombinant protein purification

GST fusion proteins were produced in *E. coli* BL21 cells transformed with the appropriate pGEX-4T-1 plasmids containing GST fusion constructs. Cells were grown to A_{600} between 0.6 and 0.8 and then induced with 1 mM isopropyl β-D-1-thiogalactopyranoside for 3–4 h at 30°C. Cells were spun down and pellets were washed with 150 mM NaCl before lysis in a buffer containing 50 mM Tris, 5 mM EDTA, 150 mM NaCl, 10% glycerol, 5 mM DTT, Pierce protease inhibitor tab, and 1 mM PMSF. Triton X-100 was added to cells in lysis buffer at a final concentration of 1%, and the lysate was incubated

on ice for 30 min. The lysate was spun at 5200 × *g* for 30 min, followed by ultracentrifugation of the supernatant at 257,000 × *g* for 1 h. Pierce glutathione agarose beads were equilibrated with PBS and 1 mM DTT, and lysate was incubated with beads for 2 h at 4°C. Beads were washed once in wash buffer containing PBS, 1 mM DTT, and 0.1% Tween, followed by a wash in wash buffer with 300 mM NaCl, before a final wash in PBS + 1 mM DTT + 150 mM NaCl. GST fusion proteins were then eluted from the beads in 50 mM Tris, pH 8.0, 150 mM NaCl, 1 mM DTT, and 25 mM glutathione and dialyzed overnight against TBS to remove free glutathione.

Statistics and data analysis

Statistical and graphical analyses were performed using GraphPad Prism 5 software. Statistical tests were chosen based on the experimental sample size, distribution, and conditions. For statistical analysis of the fixed-cell immunofluorescence imaging data, two-tailed chi-square tests, one-way analysis of variance (ANOVA), and two-sided Student's *t* test were used as appropriate. Multiple comparisons were corrected by the Bonferroni method. A p value of <0.05 was considered statistically significant. The figures and visuals were constructed in Adobe Photoshop CS6.

ACKNOWLEDGMENTS

We thank Marlena Darr and Zara Weinberg, Shanna Bowersox, and Cary Shiwarski for technical help and comments. We thank Nathan Urban, Adam Linstedt, Tina Lee, Peter Friedman, Guillermo Romero, Jean-Pierre Vilardaga, and Alessandro Bisello for reagents, comments, and suggestions. M.A.P. was supported by National Institutes of Health DA036086 and GM117425. S.E.C. was supported by a National Science Foundation Graduate Research Fellowship under Grant DGE 1256260.

REFERENCES

Arakel EC, Brandenburg S, Uchida K, Zhang H, Lin Y, Kohl T, Schrul B, Sulkin MS, Efimov IR, Nichols CG, *et al.* (2014). Tuning the electrical properties of the heart by differential trafficking of KATP ion channel complexes. J Cell Sci 127, 2106–2119.

Bao L, Jin SX, Zhang C, Wang LH, Xu ZZ, Zhang FX, Wang LC, Ning FS, Cai HJ, Guan JS, *et al.* (2003). Activation of delta opioid receptors induces receptor insertion and neuropeptide secretion. Neuron 37, 121–133.

Bie B, Zhang Z, Cai YQ, Zhu W, Zhang Y, Dai J, Lowenstein CJ, Weinman EJ, Pan ZZ (2010). Nerve growth factor-regulated emergence of functional-opioid receptors. J Neurosci 30, 5617–5628.

Bowman SL, Puthenveedu MA (2015). Postendocytic sorting of adrenergic and opioid receptors: new mechanisms and functions. Prog Mol Biol Transl Sci 132, 189–206.

Bowman SL, Shiwarski DJ, Puthenveedu MA (2016). Distinct G protein–coupled receptor recycling pathways allow spatial control of downstream G protein signaling. J Cell Biol 214, 797–806.

Bowman SL, Soohoo AL, Shiwarski DJ, Schulz S, Pradhan AA, Puthenveedu MA (2015). Cell-autonomous regulation of Mu-opioid receptor recycling by substance P. Cell Rep 24, 1925–1936.

Brock C, Boudier L, Maurel D, Blahos J, Pin JP (2005). Assembly-dependent surface targeting of the heterodimeric GABAB receptor is controlled by COPI but not 14-3-3. Mol Biol Cell 16, 5572–5578.

Brown RA, Domin J, Arcaro A, Waterfield MD, Shepherd PR (1999). Insulin activates the alpha isoform of class II phosphoinositide 3-kinase. J Biol Chem 274, 14529–14532.

Cahill CM, McClellan KA, Morinville A, Hoffert C, Hubatsch D, O'Donnell D, Beaudet A (2001). Immunohistochemical distribution of delta opioid receptors in the rat central nervous system: evidence for somatodendritic labeling and antigen-specific cellular compartmentalization. J Comp Neurol 440, 65–84.

Cahill CM, Morinville A, Hoffert C, O'Donnell D, Beaudet A (2003). Up-regulation and trafficking of delta opioid receptor in a model of chronic inflammation: implications for pain control. Pain 101, 199–208.

Cunningham MR, McIntosh KA, Pediani JD, Robben J, Cooke AE, Nilsson M, Gould GW, Mundell S, Milligan G, Plevin R (2012). Novel role for proteinase-activated receptor 2 (PAR2) in membrane trafficking of proteinase-activated receptor 4 (PAR4). J Biol Chem 287, 16656–16669.

Cvejic S, Devi LA (1997). Dimerization of the delta opioid receptor: implication for a role in receptor internalization. J Biol Chem 272, 26959–26964.

Décaillot FM, Rozenfeld R, Gupta A, Devi LA (2008). Cell surface targeting of mu-delta opioid receptor heterodimers by RTP4. Proc Natl Acad Sci USA 105, 16045–16050.

Domin J, Pages F, Volinia S, Rittenhouse SE, Zvelebil MJ, Stein RC, Waterfield MD (1997). Cloning of a human phosphoinositide 3-kinase with a C2 domain that displays reduced sensitivity to the inhibitor wortmannin. Biochem J 326, 139–147.

Dong C, Filipeanu CM, Duvernay MT, Wu G (2007). Regulation of G protein–coupled receptor export trafficking. Biochim Biophys Acta 1768, 853–870.

Duvernay MT, Dong C, Zhang X, Robitaille M, Hébert TE, Wu G (2009). A single conserved leucine residue on the first intracellular loop regulates ER export of G protein–coupled receptors. Traffic 10, 552–566.

Duvernay MT, Zhou F, Wu G (2004). A conserved motif for the transport of G protein–coupled receptors from the endoplasmic reticulum to the cell surface. J Biol Chem 279, 30741–30750.

Eichel K, von Zastrow M (2018). Subcellular organization of GPCR signaling. Trends Pharmacol Sci 39, 200–208.

Gendron L, Cahill CM, Zastrow M, Von Schiller PW, Pineyro G (2016). Molecular pharmacology of δ-opioid receptors. Pharmacol Rev 68, 631–700.

Georgoussi Z, Georganta EM, Milligan G (2012). The other side of opioid receptor signalling: regulation by protein–protein interaction. Curr Drug Targets 13, 80–102.

Gilbert CE, Zuckerman DM, Currier PL, Machamer CE (2014). Three basic residues of intracellular loop 3 of the beta-1 adrenergic receptor are required for golgin-160-dependent trafficking. Int J Mol Sci 15, 2929–2945.

Henry AG, White IJ, Marsh M, von Zastrow M, Hislop JN (2011). The role of ubiquitination in lysosomal trafficking of δ-opioid receptors. Traffic 12, 170–184.

Hermosilla R, Oueslati M, Donalies U, Schönenberger E, Krause E, Oksche A, Rosenthal W, Schülein R (2004). Disease-causing V2 vasopressin receptors are retained in different compartments of the early secretory pathway. Traffic 5, 993–1005.

Irannejad R, Pessino V, Mika D, Huang B, Wedegaertner PB, Conti M, von Zastrow M (2017). Functional selectivity of GPCR-directed drug action through location bias. Nat Chem Biol 13, 799–806.

Irannejad R, Tomshine JC, Tomshine JR, Chevalier M, Mahoney JP, Steyaert J, Rasmussen SGF, Sunahara RK, El-Samad H, Huang B (2013). Conformational biosensors reveal GPCR signalling from endosomes. Nature 495, 534–538.

Jordan BA, Devi LA (1999). G-protein–coupled receptor heterodimerization modulates receptor function. Nature 399, 697–700.

Kim K, von Zastrow M (2003). Neurotrophin-regulated sorting of opioid receptors in the biosynthetic pathway of neurosecretory cells. J Neurosci 23, 2075–2085.

Knight ZA (2011). Small molecule inhibitors of the PI3-kinase family BT. In Phosphoinositide 3-Kinase in Health and Disease: Vol. 2, ed. C Rommel, B Vanhaesebroeck, and PK Vogt, Berlin: Springer, 263–278.

Law PY, Erickson-Herbrandson LJ, Zha QQ, Solberg J, Chu J, Sarre A, Loh HH (2005). Heterodimerization of μ- and δ-opioid receptors occurs at the cell surface only and requires receptor–G protein interactions. J Biol Chem 280, 11152–11164.

Leskelä TT, Markkanen PMH, Pietilä EM, Tuusa JT, Petäjä-Repo UE (2007). Opioid receptor pharmacological chaperones act by binding and stabilizing newly synthesized receptors in the endoplasmic reticulum. J Biol Chem 282, 23171–23183.

Ma D, Zerangue N, Lin YF, Collins A, Yu M, Jan YN, Jan LY (2001). Role of ER export signals in controlling surface potassium channel numbers. Science 291, 316–319.

Magalhaes AC, Dunn H, Ferguson SS (2012). Regulation of GPCR activity, trafficking and localization by GPCR-interacting proteins. Br J Pharmacol 165, 1717–1736.

Marchese A, Paing MM, Temple BRS, Trejo J (2008). G protein–coupled receptor sorting to endosomes and lysosomes. Annu Rev Pharmacol Toxicol 48, 601–629.

Margeta-Mitrovic M, Jan YN, Jan LY (2000). A trafficking checkpoint controls GABA(B) receptor heterodimerization. Neuron 27, 97–106.

McVey M, Ramsay D, Kellett E, Rees S, Wilson S, Pope AJ, Milligan G (2001). Monitoring receptor oligomerization using time-resolved fluorescence resonance energy transfer and bioluminescence resonance energy transfer. The human delta-opioid receptor displays constitutive

oligomerization at the cell surface, which is not regulated by receptor occupancy. J Biol Chem 276, 14092–14099.
Michelsen K, Yuan H, Schwappach B (2005). Hide and run. EMBO Rep 6, 717–722.
Mittal N, Roberts K, Pal K, Bentolila LA, Fultz E, Minasyan A, Cahill C, Pradhan A, Conner D, DeFea K, *et al*. (2013). Select G-protein coupled receptors modulate agonist-induced signaling via a ROCK, LIMK and β-arrestin 1 pathway. Cell Rep 5.
Patwardhan AM, Berg KA, Akopain AN, Jeske NA, Gamper N, Clarke WP, Hargreaves KM (2005). Bradykinin-induced functional competence and trafficking of the δ-opioid receptor in trigeminal nociceptors. J Neurosci 25, 8825–8832.
Pavlos NJ, Friedman PA (2017). GPCR signaling and trafficking: the long and short of it. Trends Endocrinol Metab 28, 213–226.
Petaja-Repo UE, Hogue M, Laperriere A, Walker P, Bouvier M (2000). Export from the endoplasmic reticulum represents the limiting step in the maturation and cell surface expression of the human delta opioid receptor. J Biol Chem 275, 13727–13736.
Petäjä-Repo UE, Hogue M, Bhalla S, Laperrière A, Morello JP, Bouvier M (2002a). Ligands act as pharmacological chaperones and increase the efficiency of delta opioid receptor maturation. EMBO J 21, 1628–1637.
Petäjä-Repo UE, Hogue M, Bhalla S, Laperrière A, Morello JP, Bouvier M (2002b). Ligands act as pharmacological chaperones and increase the efficiency of delta opioid receptor maturation. EMBO J 21, 1628–1637.
Petäjä-Repo UE, Hogue M, Leskelä TT, Markkanen PMH, Tuusa JT, Bouvier M (2006). Distinct subcellular localization for constitutive and agonist-modulated palmitoylation of the human delta opioid receptor. J Biol Chem 281, 15780–15789.
Pettinger L, Gigout S, Linley JE, Gamper N (2013). Bradykinin controls pool size of sensory neurons expressing functional δ-opioid receptors. J Neurosci 33, 10762–10771.
Powis G, Bonjouklian R, Berggren MM, Gallegos A, Abraham R, Ashendel C, Zalkow L, Matter WF, Dodge J, Grindey G, *et al*. (1994). Wortmannin, a potent and selective inhibitor of phosphatidylinositol-3-kinase. Cancer Res 54, 2419–2423.
Puthenveedu MA, Lauffer B, Temkin P, Vistein R, Carlton P, Thorn K, Taunton J, Weiner OD, Parton RG, Von Zastrow M (2010). Sequence-dependent sorting of recycling proteins by actin-stabilized endosomal microdomains. Cell 143, 761–773.
Roth BL, Laskowski MB, Coscia CJ (1981). Evidence for distinct subcellular sites of opiate receptors. Demonstration of opiate receptors in smooth microsomal fractions isolated from rat brain. J Biol Chem 256, 10117–10123.
Roth D, Lynes E, Riemer J, Hansen HG, Althaus N, Simmen T, Ellgaard L (2009). A di-arginine motif contributes to the ER localization of the type I transmembrane ER oxidoreductase TMX4. Biochem J 425, 195–205.
Salahpour A, Angers S, Mercier JF, Lagacé M, Marullo S, Bouvier M (2004). Homodimerization of the β2-adrenergic receptor as a prerequisite for cell surface targeting. J Biol Chem 279, 33390–33397.
Schutze MP, Peterson PA, Jackson MR (1994). An N-terminal double-arginine motif maintains type II membrane proteins in the endoplasmic reticulum. EMBO J 13, 1696–1705.
Scott DB, Blanpied TA, Swanson GT, Zhang C, Ehlers MD (2001). An NMDA receptor ER retention signal regulated by phosphorylation and alternative splicing. J Neurosci 21, 3063–3072.
Shiwarski DJ, Darr M, Telmer CA, Bruchez MP, Puthenveedu MA (2017b). PI3K class II α regulates δ-opioid receptor export from the *trans*-Golgi network. Mol Biol Cell 28, 2202–2219.
Shiwarski DJ, Tipton A, Giraldo MD, Schmidt BF, Gold MS, Pradhan AA, Puthenveedu MA (2017a). A PTEN-regulated checkpoint regulates surface delivery of delta opioid receptors. J Neurosci 37, 3741–3752.
St-Louis É, Degrandmaison J, Grastilleur S, Génier S, Blais V, Lavoie C, Parent JL, Gendron L (2017). Involvement of the coatomer protein complex I in the intracellular traffic of the delta opioid receptor. Mol Cell Neurosci 79, 53–63.
Stoeber M, Jullie D, Lobingier BT, Laeremans T, Steyaert J, Schiller PW, Manglik A, von Zastrow M (2018). A genetically encoded biosensor reveals location bias of opioid drug action. Neuron 98, 963–976.
Vistein R, Puthenveedu MA (2013). Reprogramming of G protein–coupled receptor recycling and signaling by a kinase switch. Proc Natl Acad Sci USA 110, 15289–15294.
Wang H, Pickel VM (2001). Preferential cytoplasmic localization of delta-opioid receptors in rat striatal patches: comparison with plasmalemmal mu-opioid receptors. J Neurosci 21, 3242–3250.
Weinberg ZY, Zajac AS, Phan T, Shiwarski DJ, Puthenveedu MA (2017). Sequence-specific regulation of endocytic lifetimes modulates arrestin-mediated signaling at the m opioid receptor s. Mol Pharmacol 91, 416–427.
Whistler JL, Enquist J, Marley A, Fong J, Gladher F, Tsuruda P, Murray SR, Von Zastrow M (2002). Modulation of postendocytic sorting of G protein–coupled receptors. Science 297, 615–620.
Yuan H, Michelsen K, Schwappach B (2003). 14-3-3 dimers probe the assembly status of multimeric membrane proteins. Curr Biol 13, 638–646.
Zerangue N, Malan MJ, Fried SR, Dazin PF, Jan YN, Jan LY, Schwappach B (2001). Analysis of endoplasmic reticulum trafficking signals by combinatorial screening in mammalian cells. Proc Natl Acad Sci USA 98, 2431–2436.
Zerangue N, Schwappach B, Jan YN, Jan LY, Isaac JTR, Roche KW (1999). A new ER trafficking signal regulates the subunit stoichiometry of plasma membrane K(ATP) channels. Neuron 22, 537–548.
Zhang M, Davis JE, Li C, Gao J, Huang W, Lambert NA, Terry AV, Wu G (2016). GGA3 Interacts with a G protein–coupled receptor and modulates its cell surface export. Mol Cell Biol 36, 1152–1163.
Zhang X, Dong C, Wu QJ, Balch WE, Wu G (2011). Di-acidic motifs in the membrane-distal C termini modulate the transport of angiotensin II receptors from the endoplasmic reticulum to the cell surface. J Biol Chem 286, 20525–20535.